

Article

Characterization of Hybrid-nano/Paraffin Organic Phase Change Material for Thermal Energy Storage Applications in Solar Thermal Systems

Manoj Kumar Pasupathi ^{1,*}, Karthick Alagar ², Michael Joseph Stalin P ³,
Matheswaran M.M ⁴ and Ghosh Aritra ^{5,6,7,*}

¹ Department of Mechanical Engineering, KPR Institute of Engineering and Technology, Coimbatore 641407, India

² Department of Electrical and Electronics Engineering, KPR Institute of Engineering and Technology, Coimbatore 641407, India; karthick.a@kpriet.ac.in

³ Department of Mechanical Engineering, Audisankara College of Engineering & Technology, Gudur 524101, India; hod.me@audisankara.ac.in

⁴ Department of Mechanical Engineering, Jansons Institute of Technology, Coimbatore 641659, India; matheswaran.m@jit.ac.in

⁵ Environment and Sustainability Institute, University of Exeter, Penryn, Cornwall TR10 9FE, UK

⁶ College of Engineering, Mathematics and Physical Sciences, Renewable Energy, University of Exeter, Cornwall TR10 9FE, UK

⁷ Renewable Energy, Stella Turk Building, University of Exeter, Penryn, Cornwall TR10 9FE, UK

* Correspondence: manojkumar.p@kpriet.ac.in (M.K.P.); a.ghosh@exeter.ac.uk (G.A.)

Received: 27 August 2020; Accepted: 25 September 2020; Published: 29 September 2020



Abstract: In this work, the experimental investigations were piloted to study the influence of hybrid nanoparticles containing SiO₂ and CeO₂ nanoparticles on thermo-physical characteristics of the paraffin-based phase change material (PCM). Initially, the hybrid nanoparticles were prepared by blending equal mass of SiO₂ and CeO₂ nanoparticles. The hybrid-nano/paraffin (HnP) samples were prepared by cautiously dispersing 0, 0.5, 1.0, and 2.0 percentage mass of hybrid nanoparticles inside the paraffin, respectively. The synthesized samples were examined under different instruments such as field emission scanning electron microscope (FESEM), Fourier transform infrared spectrometer (FTIR), differential scanning calorimetry (DSC), thermogravimetric analyzer (TGA), and thermal properties analyzer to ascertain the influence of hybrid nanoparticles on thermo-physical characteristics of the prepared samples. The obtained experimental results proved that the hybrid nanoparticles were uniformly diffused in the paraffin matrix without affecting the chemical arrangement of paraffin molecules. Prominently, the relative thermal stability and relative thermal conductivity of the paraffin were synergistically enriched up to 115.49% and 165.56%, respectively, when dispersing hybrid nanoparticles within paraffin. Furthermore, the hybrid nanoparticles appropriately amended the melting and crystallization point of the paraffin to reduce its supercooling, and the maximum reduction in supercooling was ascertained as 35.81%. The comprehensive studies indicated that the paraffin diffused with SiO₂ and CeO₂ hybrid nanoparticles at 1.0 mass percentage would yield a better outcome compared to the next higher mass fractions without much diminishing the latent heat of paraffin. Hence, it is recommended to utilize the hybrid-nano/paraffin with 1.0 mass fraction of the aforementioned hybrid nanoparticles for effectively augmenting the thermal energy capacity of low-temperature solar thermal systems.

Keywords: hybrid nanoparticles; SiO₂ nanoparticles; CeO₂ nanoparticles; paraffin wax; nano-enhanced phase change material; thermal characterization

1. Introduction

In the present scenario, the potential deployment of solar energy has become the dominant thrust area for several researchers, because it is an abundantly available evergreen renewable source and it can be readily accessible on almost all the days in a year. Hence, the technological improvements have been explored for the last two decades to make use of the energy from the sun in an appreciable manner. Amid the different methods of tapping-out solar energy, the solar thermal conversion is widely employed in various scales, right from the domestic water heating to huge power plants due to their relative benefits. Particularly, the low and medium-temperature application of solar energy in water and air heating systems for domestic and industrial purposes is diffusing across the world at a faster pace [1,2]. As mentioned, solar energy is plentifully available, nonetheless, it is also having a setback that the energy is utterly weather and climate dependent due to the fluctuating manner of solar radiation. Hence, the need for supplying energy during the required period is perplexing trade at all the time. Recently, several works have been carried out by a quite a few researchers to address this problem by integrating the solar thermal systems with suitable thermal energy storage material [3].

The thermal storage materials are available in diverse forms such as sensible heat-storing materials, latent heat-storing materials using organic and inorganic compounds, and chemical energy storage [4]. Amongst the different type of thermal storage materials, latent heat storage materials are considered to be unique, as they are capable of storing more energy within a small temperature range by means of their phase transition. A broad number of phase-changing materials (PCMs) including organic and inorganic compounds have been reviewed and deliberated [5,6]. Inorganic PCMs such as molten salts have been extensively used in earlier days for the solar thermal applications due to their high latent heat capacity, however they found to have some adverse issues such as corrosiveness, instability, large supercooling and high cost. The aforementioned hitches in inorganic PCMs urged the researchers to study and experiment the other kind of materials, specifically organic PCMs, as they have been proven to possess a better fidelity with solar thermal systems [7–9]. Organic PCMs are well-known for their excellent thermo-physical properties such as significant energy density, low thermal expansion, great latent heat, chemical fidelity, thermal stability, non-corrosive and cheap availability. Nevertheless, its inferior thermal conductivity is the dominant concern, which slows down their heat transfer rate while integrating them with solar thermal systems [10,11]. This problem is appropriately addressed in different methods; placing highly conductive metallic fins inside the PCM containers, dispersing metal particles with the PCM, integrating metal foams with the PCM, and dispersing nanoparticles with high thermal conductivity in PCM [12,13]. The recent review papers [14,15] and experimental studies [16,17] evidenced the prospective of highly conductive metal, metal oxide, and carbon-based nanoparticles to augment the thermal properties of organic phase changing compounds. Li [8] admitted that relative thermal conductivity was amplified to a greater extent when a 10% nano-graphite was dispersed in paraffin. Sharma et al. [9] conducted a study on palmitic acid by adding TiO₂ nanoparticles in four mass ratios such as 0.5%, 1%, 3%, and 5%. They ascertained that TiO₂ nanoparticles enriched the chemical stability, thermal constancy, and thermal conductivity of the palmitic acid without affecting phase shift temperature and latent content of base material. In another study, paraffin was diffused with Al₂O₃ nanoparticles and stabilized with sodium stearoyl lactylate. The results publicized that the addition of Al₂O₃ nanoparticles improved the effective thermal conductivity of the paraffin up to 31%. However, the heat storage capacity of paraffin was remarkably reduced when increasing the mass fraction of Al₂O₃ nanoparticles above 5% [18].

Mohamed et al. [19] examined the thermal storage characteristics of two categories of waxes namely paraffin and microcrystalline waxes by embedding them with 0.5%, 1%, and 2% weight of α -nano alumina. They concluded that the paraffin waxes are superior to other forms of wax due to their dual phase shift behavior, and further, they reported that using the low weight of α -nano alumina with the paraffin would contribute a better improvement for low temperature solar thermal applications. Aslfattahi [20] examined the prospects of a new kind of nanoparticle called MXene at a low weight fraction to augment the thermal storage characteristics of the paraffin. MXene is the titanium carbide

nanoparticles, which have been used in three weight fractions: 0.1%, 0.2% and 0.3% weight in paraffin. They found that the 0.3% weight of nanoparticles boosted the specific heat capacity and the thermal conductivity of the base PCM by 43% and 16%, respectively, which was the maximum enhancement they had obtained through the experiments. Kumar et al. [21] acknowledged 101.67% advancement in thermal conductivity of the paraffin when it is doped with titania nanoparticles at low mass concentration. Karthick et al. [22–24] investigated the eutectic mixture of the inorganic phase change material for the building integrated photovoltaic module. It was concluded that the performance of the system improved compared to the reference system.

Relatively, a study on thermal storage behavior of paraffin-based PCM reported that by infusing a hybrid-nano containing CuO and TiO₂ nanoparticles within the paraffin had drastically suppressed cooling and heating rates owing to their colloidal behavior [25]. Alluringly, a very recent study on characterization of nano-enhanced PCM (NEPCM) using 1-dodecanol as the base PCM, once again strongly affirmed the synergistic nature of hybrid nanoparticles to advance the thermo-physical properties of PCMs, where the authors experimented with the different mass of copper–titania hybrid nanoparticles to enhance the thermal properties of PCM [26].

Beyond the aforementioned works on hybrid-nano PCMs, the comprehensive study on the influence of any other hybrid nanoparticles on thermo-physical properties of the paraffin is rarely found in any literature. A contemporary experimental analysis evidenced that the thermal properties of the paraffin were enriched by dispersing the low mass percentage of SiO₂ nanoparticles in it [27]. In a related recent study, low concentration CeO₂ nanoparticles were ascertained to a potential member to improve the thermal conductivity of water, which had been circulated in a flat plate collector (FPC) type solar water heater as a heat transfer fluid [28].

The present work is attempting to comprehensively analyze the variation of thermo-physical properties of paraffin wax under the influence of various mass percentages of the novel hybrid nanoparticles containing an equal mass of SiO₂ and CeO₂ nanoparticles to make it fit for the low-temperature solar thermal systems. The objective of this present work is to identify the opportunities to improve the thermal energy storage characteristics of paraffin by blending it with the aforesaid hybrid nanoparticles in different mass fractions. Further, the prepared samples have characterized by different instruments to find their variation in thermo-physical properties under the influence of hybrid nanoparticles.

2. Materials and Methods

2.1. Materials

The commercial-grade paraffin, which is majorly used in candle making industries, was used as the base PCM in this study, the reason being that this type of paraffin wax is available at the lowest cost compared to all other technical grade waxes without sacrificing the desirable thermo-physical properties. The required quantity of paraffin wax was acquired from a local supplier. Referring to the supplier's specification, the experimented paraffin has expected to melt between 57 °C and 64 °C, which is adequate for employing it in the low and medium temperature solar thermal systems.

The recent literature sturdily acknowledged the synergistic behavior of SiO₂ and CeO₂ nanoparticles through their chemical affinity and associative demeanor in augmenting the anticipated properties of the base material [29]. Hence, it was decided to explore the feasibility of this favorable hybrid-nano combination for attaining the expected enhancement in paraffin properties. SiO₂ nanoparticles with the mean diameter of 25 nm were provided by SRL Pvt. Ltd., Mumbai, India, and CeO₂ nanoparticles with the mean size of 25 nm had procured from Thermo Fisher Scientific India Private Limited, Mumbai, India. The thermal characteristics of the experimented paraffin and the nanoparticles have given in Table 1, as per the supplier's specification.

Table 1. Thermo-physical properties of experimented paraffin and used nanoparticles.

Properties	Materials		
	Paraffin Wax	SiO ₂ Nanoparticles	CeO ₂ Nanoparticles
Range of melting and solidification points (°C)	63.74	1713	2600
Physical appearance	Pellets	Powder	Powder
Colour	White	White	Pale yellow
Thermal conductivity (W/mK)	0.180	1.5	12

2.2. Preparation of Nano-Hybrid/Paraffin Samples

Hybrid nanoparticles were attained by thoroughly blending equal mass SiO₂ and CeO₂ nanoparticles in a clean container. Then, hybrid-nano/paraffin samples have been synthesized by carefully disbanding 0%, 0.5%, 1.0%, and 2.0% mass of prepared hybrid nanoparticles in molten paraffin as mentioned in Table 2. The aforementioned progressive mass fractions had been chosen to rely on the recommendations from the preceding studies, as it was proclaimed that the nanoparticles are giving their maximum benefits at low mass fractions because they begin to agglomerate, diminish the latent heat, increase the material cost relative to their mass fraction selection [19,30,31].

Table 2. Mass of different constituents in nano-hybrid/paraffin samples.

S.No.	Sample Name	Composition in Mass (Grams)
1.	Pure paraffin	100 paraffin
2.	0.5 HnP	99.5 paraffin + 0.25 SiO ₂ nanoparticles + 0.25 CeO ₂ nanoparticles
3.	1.0 HnP	99 paraffin + 0.5 SiO ₂ nanoparticles + 0.5 CeO ₂ nanoparticles
4.	2.0 HnP	98 paraffin + 1.0 SiO ₂ nanoparticles + 1.0 CeO ₂ nanoparticles

The hybrid-nano/paraffin samples were prepared using two-step method, as in the study piloted by Kumar et al. [32]. The paraffin wax was melted in a bath containing hot water and carefully transferred to a magnetic stirrer. Subsequently, the aforementioned hybrid nanoparticles of the essential mass were added carefully to the molten paraffin wax at the steady rate, and simultaneously heated and stirred on the magnetic stirrer for two hours to obtain a homogeneous mixture. Further, the composite mixture was sonicated for sixty minutes using an ultrasonicator to obtain the fine dispersion of the nanoparticles in paraffin. The surfactant was not utilized in this study to elude their effect on the thermal conductivity of the hybrid-nano/paraffin [33]. The prepared hybrid-nano/paraffin samples were then molded into the cylindrical form as exhibited in Figure 1.

2.3. Investigations on Thermo-Physical Properties of Nano-Hybrid/Paraffin Samples

The synthesized HnP samples with four different compositions were examined for their microscopic structure, thermal stability, chemical stability, melting and solidification temperature, supercooling nature, latent heat, and thermal conductivity, which decide heat storage characteristics of the PCM.

The particle size of the commercially procured SiO₂ and CeO₂ nanoparticles was verified using Zetasizer AT supplied by Malvern Panalytical Ltd, Malvern, UK. The degree of dispersion of hybrid nanoparticles within the paraffin matrix was analyzed by employing a Zeiss Sigma field emission scanning electron microscope (FESEM) made by Carl Zeiss Microscopy GmbH, Oberkochen, Germany. The chemical stability of the hybrid-nano/paraffin samples was investigated with a Spectrum two FT-IR from PerkinElmer, Massachusetts, United State. Further, thermal properties such as melting temperature, crystallization temperature, degree of supercooling, and latent heat capacity of the hybrid-nano/paraffin samples were examined with differential scanning calorimetry using a DSC 6000 with Pyris 6 DSC (PerkinElmer). The thermal stability of the samples at the higher temperature was analyzed by Thermogravimetric Analyzer (PerkinElmer thermogravimetric analyzer (TGA) 4000).

A KD2 Pro thermal properties analyzer (Make of Decagon Devices, Inc., Pullman, WA, USA) was deployed to assess the thermal conductivity of the HnP samples.

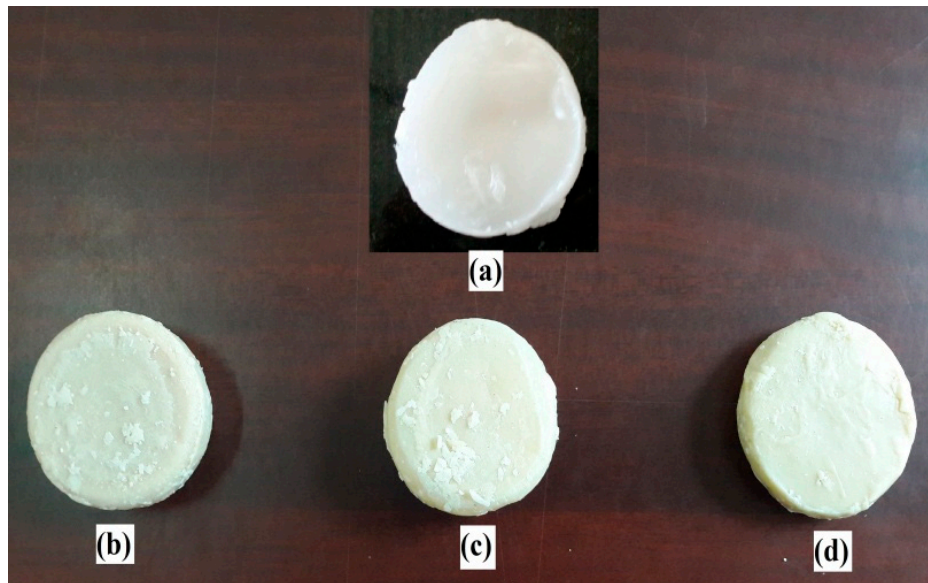


Figure 1. Molded hybrid-nano/paraffin samples. (a) Pure paraffin; (b) 0.5 HnP; (c) 1.0 HnP; (d) 2.0 HnP.

3. Results and Discussion

3.1. Validation of Nanoparticle Size and Investigating Surface Morphology of the HnP Samples

The mean particle size of SiO₂ and CeO₂ nanoparticles were examined separately by utilizing a particle size analyzer made by Zetasizer. This test was performed to ensure whether the mean size of the nanoparticles complied with the supplier's specification and to identify the percentage distribution of different sized nanoparticles that were used in the HnP samples. The results acquired after the particle size analysis on SiO₂ and CeO₂ nanoparticles are presented in Figure 2.

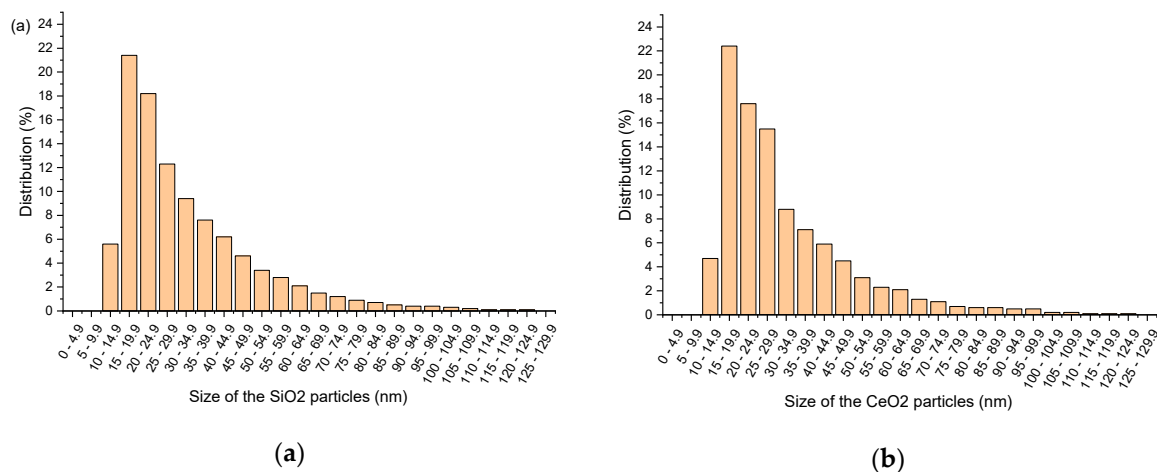


Figure 2. Size distribution of (a) SiO₂ nanoparticles (b) CeO₂ nanoparticles.

It was observed from Figure 2a that the SiO₂ nanoparticle sample contains 21.4% of particles with the size between 15 nm and 19.9 nm, which is the maximum dominant sized particles in the investigated sample. The range between 20 nm and 29.9 nm samples together stand with the percentage distribution of 30.5%. A similar result was obtained for the CeO₂ sample. The mean particle diameter between 15 nm and 19.9 nm has been noticed as the maximum distribution of 22.4%, and subsequently, 20–24.9 nm

and 25–29.9 nm samples were found to be with 17.6% and 15.5%, respectively (Figure 2b). More than 50% of both nanoparticles are in the size between 15 nm and 30 nm, which was specified by the supplier. Hence, it can be ascertained that procured nanoparticles are conforming to the supplier's description without any contradiction.

The prepared hybrid-nano/paraffin samples were inspected under FESEM, and resulting images are presented in Figure 3a–d. The samples were gold-coated for evading the growth of charge, and the imaging was accompanied by an in-lens detector, which is basically an annular secondary electron detector (SE detector) used to get the surface structure of the samples. The images were captured with a low resolution scanning for avoiding the fusion of paraffin by the high energy electron scanning, as suggested by George et al. [34].

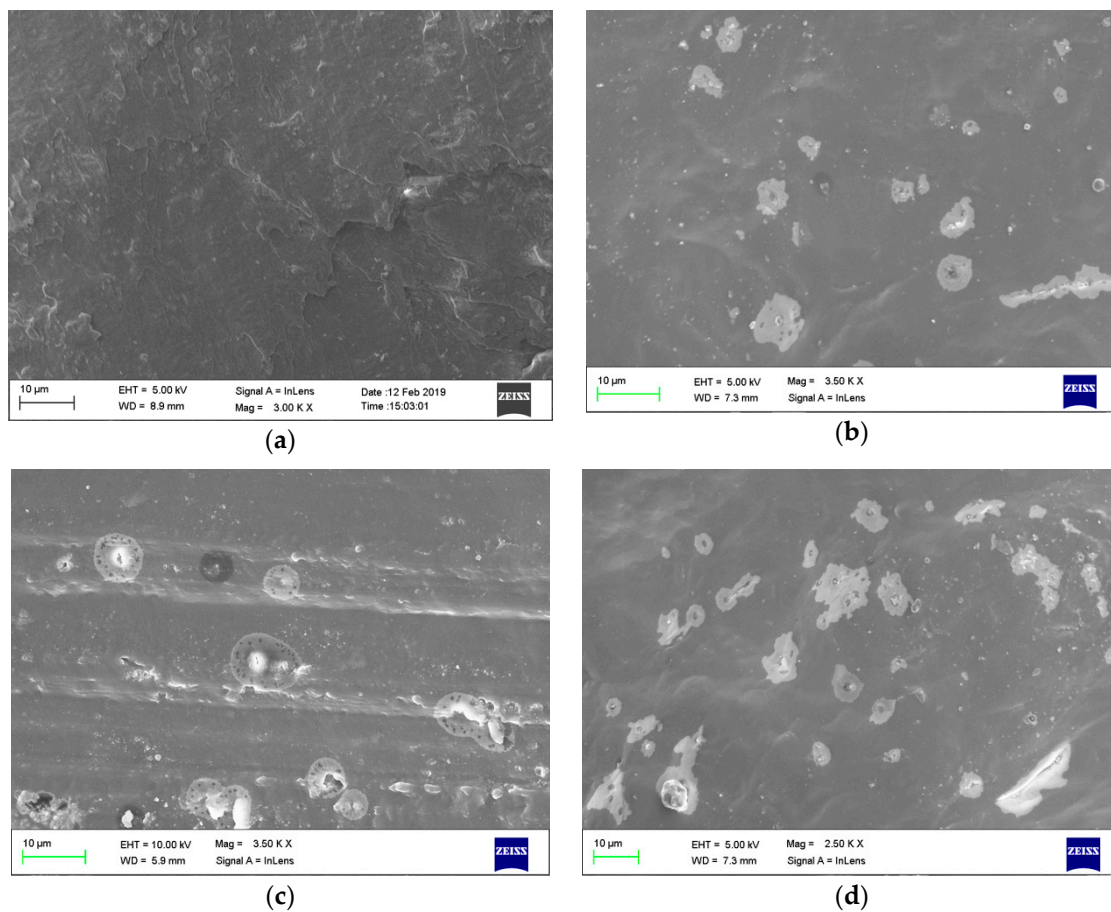


Figure 3. Field emission scanning electron microscope (FESEM) images of (a) pure paraffin, (b) 0.5 HnP, (c) 1.0 HnP, and (d) 2.0 HnP.

The resulting images (Figure 3b–d) represented the distribution of nanoparticles inside the paraffin matrix, and homogeneous nature of hybrid-nano/paraffin at the low mass fractions. It has become the evidence that the nanoparticles formed a sound physical network inside the paraffin matrix, and this network found to be stronger with the upsurge in mass% of the hybrid nanoparticles. On the other hand, the agglomeration tends to be formed while upsurging the mass of nanoparticles, which may be primarily ascribed to the Van der Waals forces among the nanoparticles complemented with the Brownian motion [35]. However, in this present investigation, the dispersion was found to have better physical interaction without substantial agglomeration in all the prepared samples, except for the sample having 2.0% of hybrid nanoparticles (Figure 3d). It was highly attributable to the sufficient sonication provided during their preparation.

3.2. Chemical Stability of the HnP Samples

The FT-IR was performed on hybrid-nano/paraffin samples to investigate the chemical compatibility between paraffin and nanoparticles in the samples. The results are presented in Figure 4a–d. The FT-IR result of pure paraffin sample (Figure 4a) has been found with the medium vibrational bands at the wavenumbers 729 cm^{-1} and 1462 cm^{-1} , which can be credited to rocking skeleton vibration of C-C groups. Besides, two major vibrational shifts at 2848 cm^{-1} and 2916 cm^{-1} , and a minor band at 2956 cm^{-1} have been identified, which can be characterized by symmetrical and asymmetrical stretching characteristics of aromatic C-H structure, respectively. The aforementioned peaks were noticed in all the HnP samples, irrespective of the blended nanoparticle composition. However, the samples having hybrid nanoparticles (Figure 4b–d) were noticed with two more small shifts at the wavenumbers 1102 cm^{-1} [36] and 521 cm^{-1} [37], which corresponds to shifting of Si-O-C functional group and stretching vibration of Ce-O group, respectively. A similar absorption spectrum was obtained for all the samples, which is the indication that the chemical arrangement of paraffin was not significantly disturbed with the loading of nano-SiO₂ and nano-CeO₂ particles and no new compounds were formed due to the interfacing of nanoparticles with paraffin. Hence, it can be ascertained that the nanoparticles were chemically inert with the paraffin and the HnP composites are feasible for repeating cycles, as they possess good chemical stability.

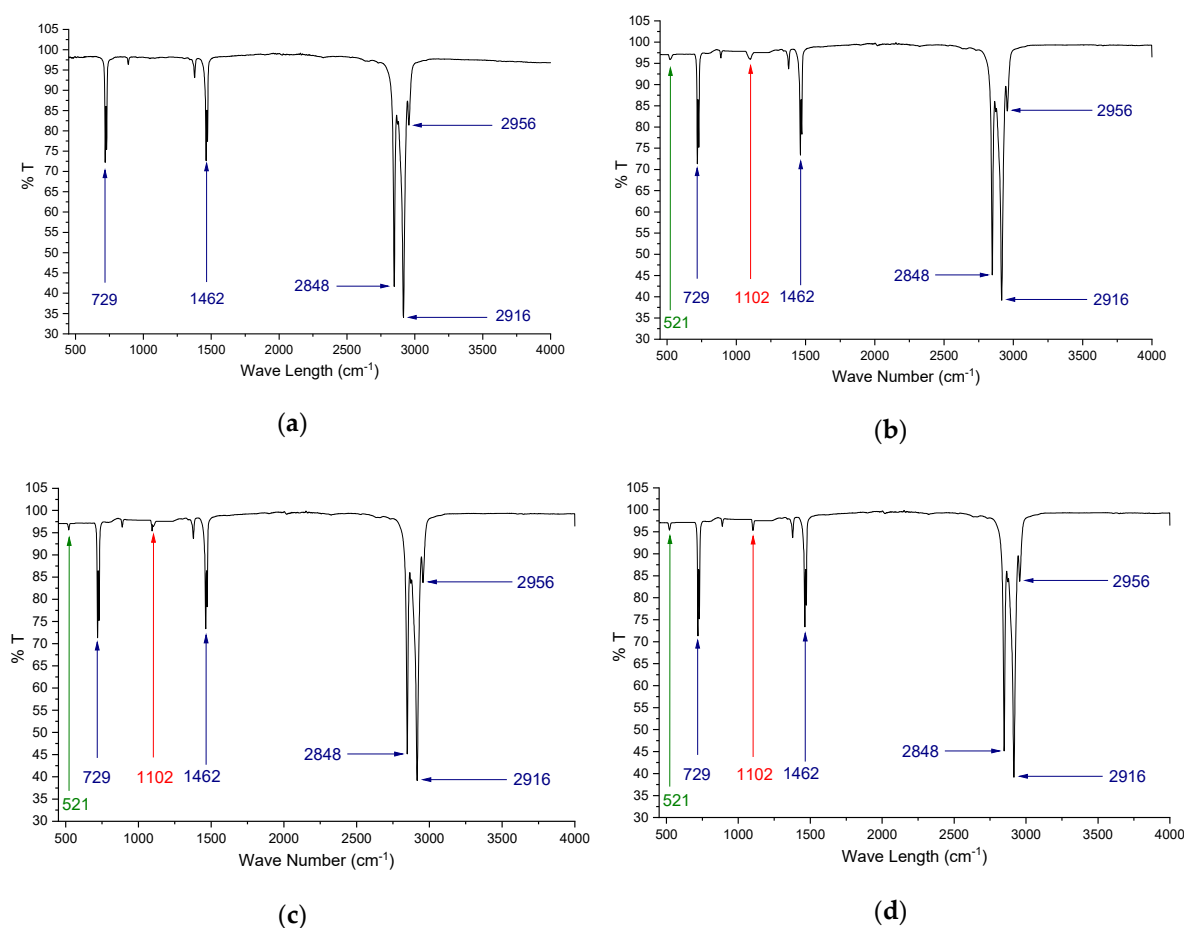


Figure 4. Fourier transform infrared spectrometer (FTIR) results of (a) Pure paraffin (b) 0.5 HnP (c) 1.0 HnP (d) 2.0 HnP.

3.3. DSC Examination of the HnP Samples

The differential scanning calorimetry (DSC) analysis was conducted on all the HnP samples at the rate of $5\text{ }^{\circ}\text{C}$ per minute in a nitrogen atmosphere and the temperature was programmed

between 30 °C and 80 °C considering the phase transition temperature of paraffin, as endorsed by Lin and Al-Kayiem [38]. The comprehensive DSC results comprising of latent heat, fusion, and crystallization temperatures of the HnP samples with 0%, 0.5%, 1.0%, and 2.0% mass of hybrid nanoparticles are given in Table 3. Further, the DSC plot for the heating and cooling of the samples is portrayed in Figure 5. It vividly demonstrates that two distinguished crests were originated during the thermal cycle for all the four HnP samples. The minor crest during the heating and cooling was owing to the transformation in the crystalline structure of the paraffin (solid–solid phase transition). Later, a substantial rise was observed in the samples, which are predominantly due to the solid to liquid phase conversion, and this large significant peak determines the thermal storage capability of the PCM in the form of latent capacity [39].

Table 3. Thermal properties of hybrid-nano/paraffin samples assessed with DSC.

Sample Name	Melting Point (°C)	Latent Heat during Melting (kJ/kg)	Thermal Properties		Degree of Supercooling (°C)
			Solidification Point (°C)	Latent Heat during Solidification (kJ/kg)	
Pure Paraffin	63.74	140.2	57.01	134.6	6.73
0.5 HnP	63.27	136.1	57.06	129.4	5.67
1.0 HnP	62.81	133.7	58.79	127.8	4.32
2.0 HnP	63.09	111.2	58.21	95.4	4.88

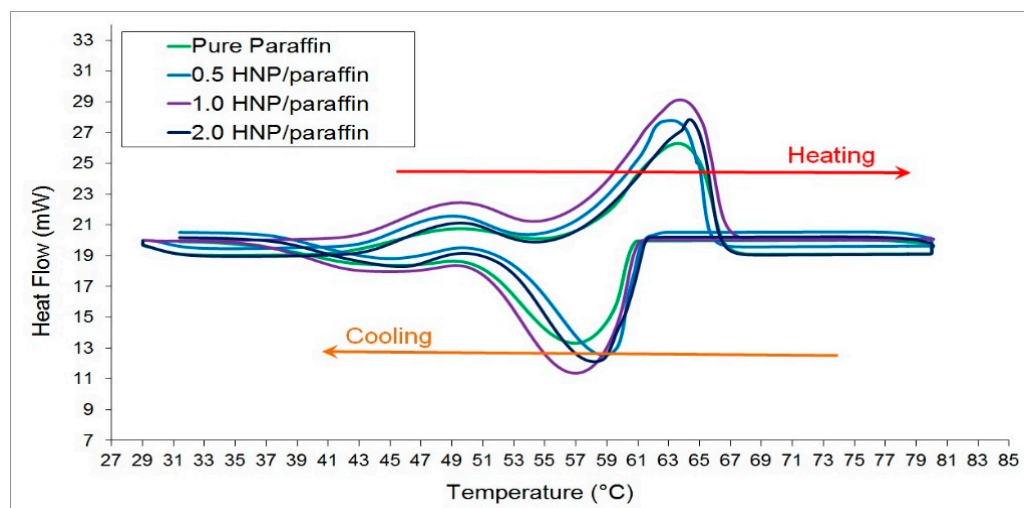


Figure 5. DSC results of the hybrid-nano/paraffin samples.

The critical investigation on melting and crystallization points and their consequences on the supercooling of the HnP samples can be exemplified with the aid of Figure 6. It could be understood that the melting point of the paraffin was shortened marginally with the addition of hybrid nanoparticles. Likewise, the solidification point of the paraffin was observably amplified with the loading of hybrid nanoparticles. This is the unblemished evidence, which authenticates that the hybrid nanoparticles repressed the supercooling of the paraffin by enhancing the rate of nucleation during cooling. The extremely beneficial alterations in crystallization and melting points were observed for the HnP sample containing 1.0 mass fraction of hybrid nanoparticles. The supercooling was rapidly abridged to 4.32 °C by this corresponding HnP sample, which is 35.81% less than that of paraffin.

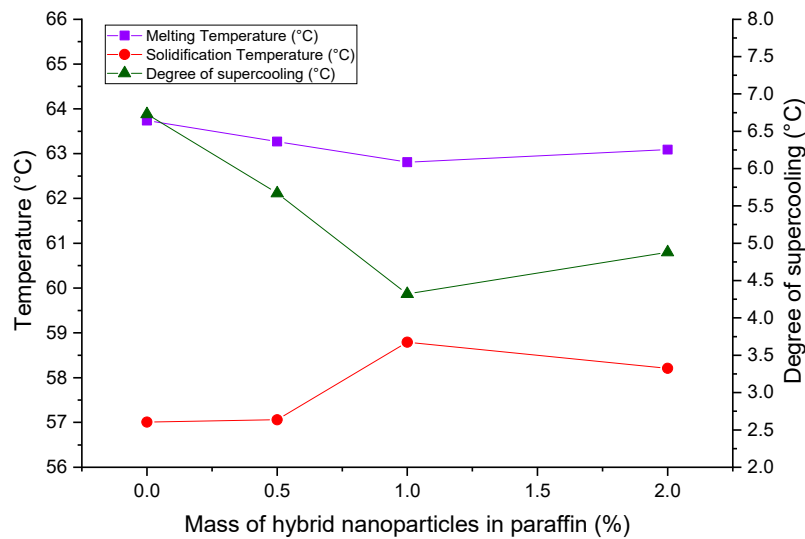


Figure 6. Variation in melting temperature, solidification temperature and degree of supercooling of hybrid-nano/paraffin.

On the contrary, the latent capacity of paraffin was diminished with the increment in mass percentage of hybrid nanoparticles, as presented in Figure 7. Nonetheless, the rate of drop in latent heat was trivial until the stocking of hybrid nanoparticles up to 1.0 mass percentage. The substantial fall in latent heat capacity was witnessed for the HnP containing 2.0 mass fraction of nanoparticles and the reduction was 20.68% and 29.12% during melting and freezing, respectively, due to the physio-chemical modifications within the composite matrix [25]. Further, the low density the HnP and reduced mass content of the paraffin have been attributed to be the prime causes for the latent heat reduction in paraffin at the higher mass fraction of nanoparticles [8,38]. Sahan and Paksoy [40] reported a like result when they dispensed a 10% weight of zinc oxide nanoparticles in the paraffin matrix. On the whole, the paraffin with 1.0 mass% of the hybrid nanoparticles designates the appreciable improvement in terms of reducing supercooling without much compromising the latent heat of paraffin, compared to the paraffin with 2.0 mass% of nanoparticles.

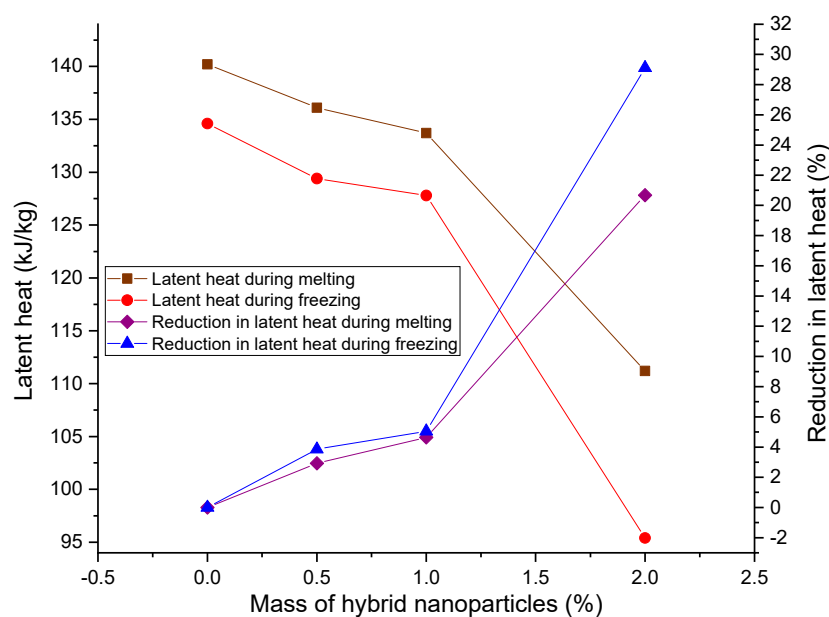


Figure 7. Variation in latent capacity of the hybrid-nano/paraffin samples.

3.4. Thermal Stability and Thermal Conductivity of the HnP Samples

Thermogravimetric analysis (TGA) was conducted for all the HnP samples to assess the thermal stability of the samples over the temperature range by determining their thermal degradation temperatures. Each sample of 5.5 mg was tested under a nitrogen atmosphere at the speed of 10 °C per minute between the temperature range of 30 °C and 450 °C [27,41]. The quantified results are plotted and presented in Figure 8. The thermal degradation of the samples with 0, 0.5, 1.0, and 2.0 percentage mass of hybrid nanoparticles were found to be originated at 142°C, 160 °C, 163 °C, and 164 °C and completed at 244 °C, 267 °C, 270 °C, and 271 °C, respectively. The degradation temperature of the paraffin was appreciably improved with the addition of HnP, as the nanoparticles enhanced the physical bonding among the paraffin molecules due to their low density [38]. Likewise, the residual mass remained after the thermal degradation of samples is observed as 0%, 0.3%, 1.1%, and 2.2%, respectively. The pure paraffin had not remained at 260 °C and all other samples with 0.5%, 1.0%, and 2.0% mass of hybrid nanoparticles were perfectly degraded at 450 °C.

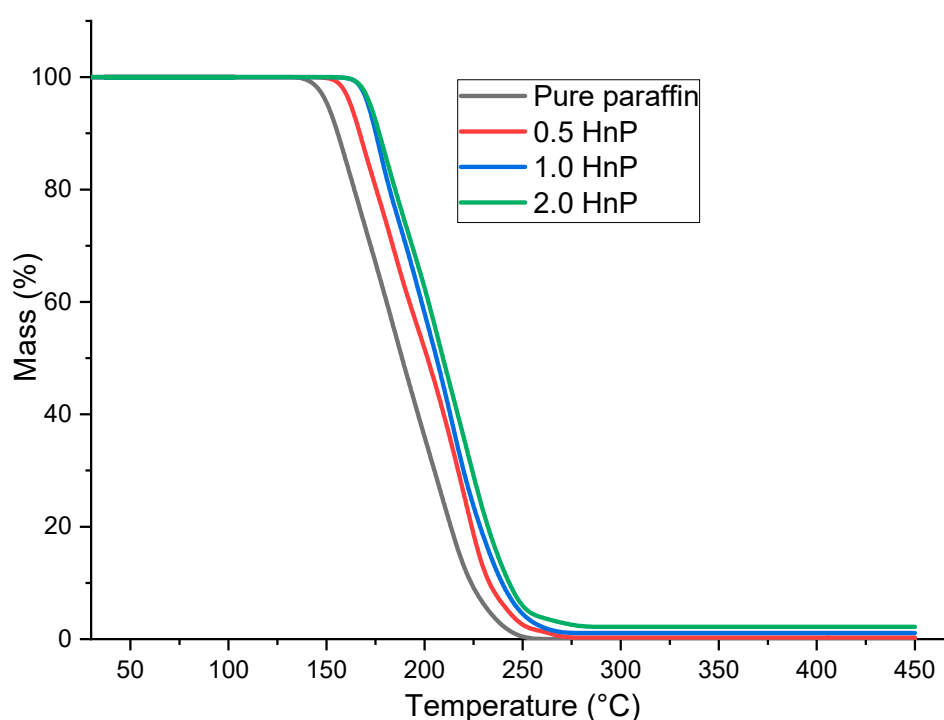


Figure 8. Thermogravimetric analyzer (TGA) plot of the hybrid-nano/paraffin samples.

It can be visibly seen that the degradation of the paraffin was prominently delayed by adding 2.0% mass of nanoparticle, which is 21 °C greater than that of pure paraffin. Nevertheless, the progress was nominal, while adding nanoparticles more than 0.5 mass fraction in paraffin. The relative thermal stability is the ratio of thermal degradation temperature of HnP to that of pure paraffin. It could also be evidence that the thermal stability of the paraffin was substantially upgraded while adding nanoparticles of 0.5 mass fraction and the enhancement was insignificant beyond it. From the TGA of the HnP samples, it is certainly inferred that the distribution of hybrid nanoparticles remarkably amended the thermal degradation of the paraffin, which is around more than twenty percent better than the available literature [39]. However, the improvement seems to be insignificant after adding 0.5 percentage mass of hybrid nanoparticles.

Thermal conductivity of paraffin and hybrid-nano/paraffin was acquired by means of a KD2 pro thermal properties analyzer, which fundamentally works on the principle of transient line heat source with a single needle sensor [42–44]. It is observed that paraffin's thermal conductivity is boosted to 0.231 W/mK, 0.26 W/mK, and 0.298 W/mK by dispersing 0.5%, 1.0%, and 2.0% mass of hybrid

nanoparticles, respectively, in paraffin, whereas thermal conductivity of pure paraffin was measured as 0.18 W/mK. The enrichment in thermal conductivity is witnessed with the increasing mass of hybrid nanoparticles in paraffin, and it seemed to be non-linear. The improved thermal conductivity can be justified as follows: Brownian motion of distinguished hybrid nanoparticles combination within paraffin improved the convective heat transfer comparatively higher than the conductive heat transfer [45], and it became the primary reason for noticeable amplification in the heat transfer rate of the base material. The measured thermal conductivity of the hybrid-nano/paraffin samples is suitably fitted, and the curves are presented in Figure 9. From the curve fitting, the correlation between the thermal conductivity of the HnP samples (k) and the mass percentage of experimented hybrid nanoparticles (x) can be obtained as

$$k = 0.18125 + 0.10435x - 0.02309x^2. \quad (1)$$

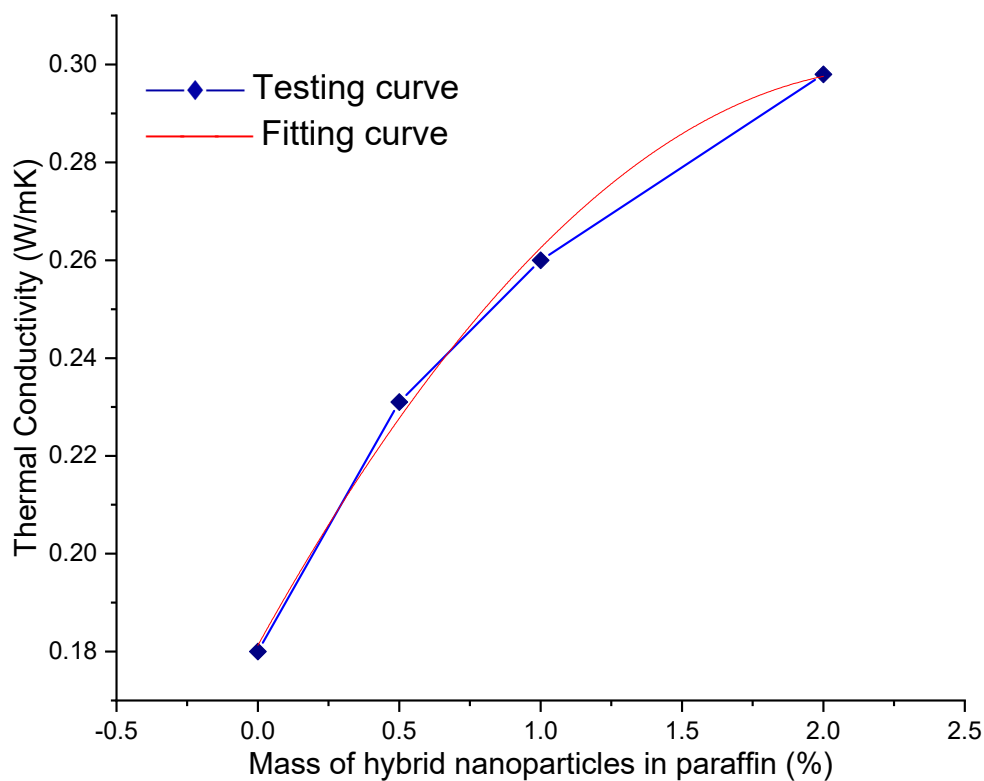


Figure 9. Thermal conductivity of the hybrid-nano/paraffin samples.

The correlation coefficient of the above equation had arrived at 0.99741. The relative value of the thermal conductivity is the ratio between the thermal conductivity of the HnP and pure paraffin [8].

Figure 10 interprets the percentage enrichment in relative thermal conductivity of the PCM with the charging of hybrid nanoparticles. The relative thermal conductivity was upsurged steadily with the stocking of nanoparticles. However, the slope seems to be reduced after the addition of 1.0 mass of nanoparticles, which is witnessed from Figure 10. Lin and Al-Kayiem [38] reported the same trend of variation in thermal conductivity when they had deployed copper nanoparticles in paraffin, and they claim that the increased mass percentage of nanoparticles in the base material, beyond a critical value, may form the irrepressible agglomeration owing to the prevailing cohesive forces, which would be the reason for the diminished slope in the magnitude of thermal conductivity at the upper mass fractions.

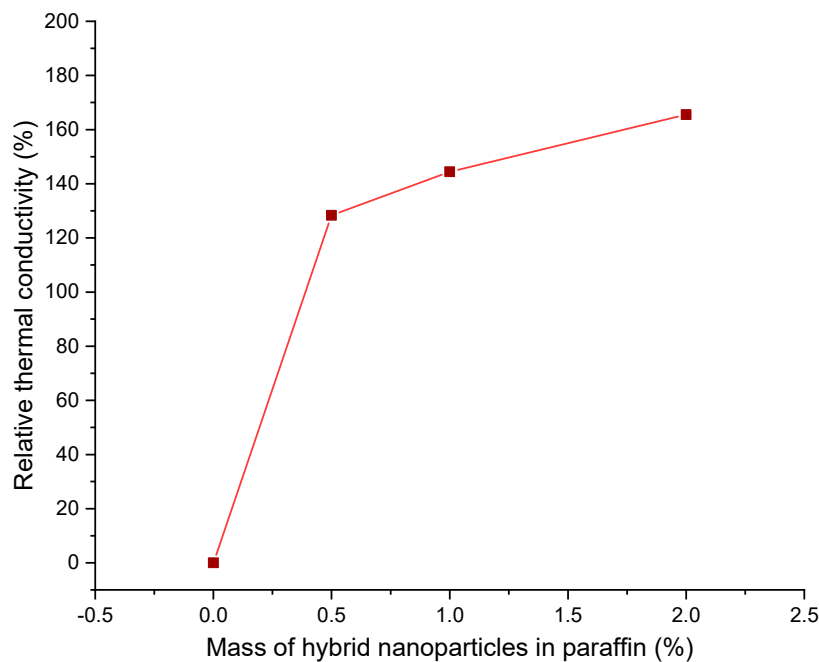


Figure 10. Relative thermal conductivity of hybrid-nano/paraffin samples.

Comparing the Figures 7 and 9, it can be explicitly understood that the trend of variation in latent heat content and thermal conductivities is completely contrary to the addition of nanoparticles. Among the experimented mass fraction of HnP, 1.0 mass fraction of hybrid nanoparticles seems to be the optimum mass percentage to obtain the maximum beneficial thermal storage characteristics of paraffin.

4. Conclusions

The four samples of paraffin-based hybrid-nano/paraffin (HnP) had prepared by diffusing 0, 0.5, 1.0, and 2.0 percentage mass of hybrid nanoparticles (nano-SiO₂ and nano-CeO₂) in paraffin, respectively. Then, the samples were experimentally investigated with the different types of instruments to assess the influence of hybrid nanoparticles on physical structure, chemical stability, and thermal properties of paraffin, which is to be engaged as a thermal storage medium for solar thermal systems. The following concluding points have arrived from the inference of the obtained results.

1. FESEM images of the samples showed that the hybrid nanoparticles were scattered evenly in the paraffin matrix, and they formed a percolated network to facilitate the effective transfer of heat. The proximity of the particle distribution was shrunk with an increasing mass percentage of nanoparticles, which leads to agglomeration. Except for 2.0 HnP, all other samples were affably homogeneous in nature.

2. DSC plots clarified that the incorporation of hybrid nanoparticles reduced the difference between melting and solidification points, which in turn suppressed the supercooling of the paraffin. Contrarily, the heaping of nanoparticles lessened the latent heat of paraffin. Nonetheless, the declination in latent heat seems to be insignificant, until the increase of 1.0 percentage mass of hybrid nanoparticles. The HnP sample containing 1.0 mass of nanoparticles appears to be superior in terms of condensed supercooling compared to other samples, which is due to the improved physio-chemical interaction between the paraffin molecules at this mass fraction of HnP.

3. Fourier transform infrared spectrometer (FTIR) results of hybrid-nano/paraffin samples exemplified the chemical inertness of the paraffin with the added hybrid nanoparticles. The nanoparticles showcased high chemical resistance between themselves and with the paraffin matrix.

4. TGA of samples witnessed that the diffusion of hybrid nanoparticles in paraffin delayed the thermal decomposition of paraffin by substantially increasing the thermal decomposition temperature of the paraffin. However, the enhancement was immaterial after the addition of 0.5 mass fraction of hybrid nanoparticles in paraffin.

5. Thermal conductivity assessments evidenced the capability of hybrid nanoparticles to augment the thermal conductivity of paraffin. Further, the thermal conductivity enrichment was less sloped after adding 1.0 mass fraction of hybrid nanoparticles inside paraffin, due to the adverse agglomeration of nanoparticles.

Conjoining the achieved results, it is obviously evidenced that the diffusion of hybrid (combination of nano-SiO₂ and nano-CeO₂) nanoparticles in paraffin at 1.0 mass percentage have shown better enhancements in the thermal storage characteristics of the paraffin compared to the next higher mass fraction, and it is recommended for the potential augmentation in thermal storage of low-temperature solar thermal systems.

Author Contributions: Conceptualization, M.K.P. and K.A.; Methodology, M.K.P. and M.M.M.; Validation, M.K.P. and K.A.; Formal analysis, G.A.; Investigation, M.M.M.; Resources, M.J.S.P.; Data curation, K.A.; Writing—original draft preparation, M.K.P.; Writing—review and editing, K.A.; Visualization, M.J.S.P.; Supervision, M.K.P.; Project administration, G.A.; Funding acquisition, M.J.S.P. All authors have read and agreed to the published version of the manuscript.

Funding: This research received no external funding.

Acknowledgments: We would like to thank KPR Institute of Engineering and Technology for the administrative support to complete our project.

Conflicts of Interest: The authors declare no conflict of interest.

References

1. Reddy, K.P.; Gupta, M.V.N.; Nundy, S.; Karthick, A.; Ghosh, A. Status of BIPV and BAPV System for Less Energy-Hungry Building in India—A Review. *Appl. Sci.* **2020**, *10*, 2337. [[CrossRef](#)]
2. Kumar, P.M.; Saravanakumar, P.T.; Mysamy, K.; Kishore, P.; Prakash, K.B. Study on thermal conductivity of the candle making wax (CMW) using nano-TiO₂ particles for thermal energy storage applications. *Aip Conf. Proc.* **2019**, *2128*, 020027.
3. Ghosh, A. Potential of building integrated and attached/applied photovoltaic (BIPV/BAPV) for adaptive less energy-hungry building's skin: A comprehensive Review. *J. Clean. Prod.* **2020**, 123343. [[CrossRef](#)]
4. Pichandi, R.; Kulandaivelu, K.M.; Alagar, K.; Dhevaguru, H.K.; Ganesamoorthy, S. Performance enhancement of photovoltaic module by integrating eutectic inorganic phase change material. *Energy Sources Part A Recovery Util. Environ. Eff.* **2020**. [[CrossRef](#)]
5. Nazir, H.; Batool, M.; Osorio, F.J.B.; Isaza-Ruiz, M.; Xu, X.; Vignarooban, K.; Phelan, P.; Kannan, A.M. Recent developments in phase change materials for energy storage applications: A review. *Int. J. Heat Mass. Tran.* **2019**, *129*, 491–523. [[CrossRef](#)]
6. Karthick, A.; Manokar Athikesavan, M.; Pasupathi, M.K.; Manoj Kumar, N.; Chopra, S.S.; Ghosh, A. Investigation of Inorganic Phase Change Material for a Semi-Transparent Photovoltaic (STPV) Module. *Energies* **2020**, *13*, 3582. [[CrossRef](#)]
7. Kumar, P.M.; Anandkumar, R.; Mysamy, K.; Prakash, K.B. Experimental investigation on thermal conductivity of nanoparticle dispersed paraffin (NDP). *Mater. Today-Proc.* **2020**. [[CrossRef](#)]
8. Li, M. A nano-graphite/paraffin phase change material with high thermal conductivity. *Appl. Energ.* **2013**, *106*, 25–30. [[CrossRef](#)]
9. Sharma, R.K.; Ganesan, P.; Tyagi, V.V.; Metselaar, H.S.C.; Sandaran, S.C. Thermal properties and heat storage analysis of palmitic acid-TiO₂ composite as nano-enhanced organic phase change material (NEOPCM). *Appl. Eng.* **2016**, *99*, 1254–1262.
10. Chen, B.; Han, M.; Zhang, B.; Ouyang, G.; Shafei, B.; Wang, X.; Hu, S. Efficient Solar-to-Thermal Energy Conversion and Storage with High-Thermal-Conductivity and Form-Stabilized Phase Change Composite Based on Wood-Derived Scaffolds. *Energies* **2019**, *12*, 1283. [[CrossRef](#)]

11. Qian, T.; Zhu, S.; Wang, H.; Li, A.; Fan, B. Comparative study of single-walled carbon nanotubes and graphene nanoplatelets for improving the thermal conductivity and solar-to-light conversion of PEG-infiltrated phase-change material composites. *ACS Sustain. Chem. Eng.* **2018**, *7*, 2446–2458. [[CrossRef](#)]
12. Liu, Z.; Zang, C.; Ju, Z.; Hu, D.; Zhang, Y.; Jiang, J.; Liu, C. Consistent preparation, chemical stability and thermal properties of a shape-stabilized porous carbon/paraffin phase change materials. *J. Clean. Prod.* **2020**, *247*, 119565. [[CrossRef](#)]
13. Lin, Y.; Jia, Y.; Alva, G.; Fang, G. Review on thermal conductivity enhancement, thermal properties and applications of phase change materials in thermal energy storage. *Renew. Sust. Energ. Rev.* **2018**, *82*, 2730–2742. [[CrossRef](#)]
14. Ahmed, S.F.; Khalid, M.; Rashmi, W.; Chan, A.; Shahbaz, K. Recent progress in solar thermal energy storage using nanomaterials. *Renew. Sust. Energ. Rev.* **2017**, *67*, 450–460. [[CrossRef](#)]
15. Qiu, L.; Ouyang, Y.; Feng, Y.; Zhang, X. Review on micro/nano phase change materials for solar thermal applications. *Renew. Energ.* **2019**, *140*, 513–538. [[CrossRef](#)]
16. Manoj Kumar, P.; Mylsamy, K.; Karthick, A.; Sudhakar, K. Investigations on an evacuated tube solar water heater using hybrid-nano based organic Phase Change Material. *Int. J Green Energy* **2020**. [[CrossRef](#)]
17. Kumar, P.M.; Anandkumar, R.; Sudarvizhi, D.; Prakash, K.B.; Mylsamy, K. Experimental investigations on thermal management and performance improvement of solar PV panel using a phase change material. *AIP Conf. Proc.* **2019**, *2128*, 020023.
18. Nourani, M.; Hamdami, N.; Keramat, J.; Moheb, A.; Shahedi, M. Thermal behavior of paraffin-nano-Al₂O₃ stabilized by sodium stearyl lactylate as a stable phase change material with high thermal conductivity. *Renew. Energ.* **2016**, *88*, 474–482. [[CrossRef](#)]
19. Mohamed, N.H.; Soliman, F.S.; El Maghraby, H.; Moustfa, Y.M. Thermal conductivity enhancement of treated petroleum waxes, as phase change material, by α nano alumina: Energy storage. *Renew. Sust. Energ. Rev.* **2017**, *70*, 1052–1058. [[CrossRef](#)]
20. Asfattahi, N.; Saidur, R.; Arifutzzaman, A.; Sadri, R.; Bimbo, N.; Sabri, M.F.M.; Maughan, P.A.; Bouscarrat, L.; Dawson, R.J.; Said, S.M.; et al. Experimental investigation of energy storage properties and thermal conductivity of a novel organic phase change material/MXene as A new class of nanocomposites. *J. Energ. Stor.* **2020**, *27*, 101115. [[CrossRef](#)]
21. Kumar, P.M.; Mylsamy, K.; Saravanakumar, P.T.; Anandkumar, R.; Pranav, A. Experimental Study on Thermal Properties of Nano-TiO₂ Embedded Paraffin (NEP) for Thermal Energy Storage Applications. *Mater. Today-Proc.* **2020**, *22*, 2153–2159. [[CrossRef](#)]
22. Karthick, A.; Ramanan, P.; Ghosh, A.; Stalin, B.; Vignesh Kumar, R.; Baranilingesan, I. Performance enhancement of copper indium diselenide photovoltaic module using inorganic phase change material. *Asia-Pac. J. Chem. Eng.* **2020**, e2480. [[CrossRef](#)]
23. Karthick, A.; Murugavel, K.K.; Ghosh, A.; Sudhakar, K.; Ramanan, P. Investigation of a binary eutectic mixture of phase change material for building integrated photovoltaic (BIPV) system. *Solar Energy Mater Solar Cells* **2020**, *207*, 110360. [[CrossRef](#)]
24. Karthick, A.; Murugavel, K.K.; Ramanan, P. Performance enhancement of a building-integrated photovoltaic module using phase change material. *Energy* **2018**, *142*, 803–812. [[CrossRef](#)]
25. Harikrishnan, S.; Deepak, K.; Kalaiselvam, S. Thermal energy storage behavior of composite using hybrid nanomaterials as PCM for solar heating systems. *J. Anal. Calorim.* **2014**, *115*, 1563–1571. [[CrossRef](#)]
26. Parameshwaran, R.; Kumar, G.N.; Ram, V.V. Experimental analysis of hybrid nanocomposite-phase change material embedded cement mortar for thermal energy storage. *J. Build. Eng.* **2020**, *30*, 101297. [[CrossRef](#)]
27. Manoj Kumar, P.; Mylsamy, K.; Saravanakumar, P.T. Experimental investigations on thermal properties of nano-SiO₂/paraffin phase change material (PCM) for solar thermal energy storage applications. *Energy Source Part A* **2019**, *42*, 2420–2433. [[CrossRef](#)]
28. Stalin, P.M.J.; Arjunan, T.V.; Matheswaran, M.M.; Sadanandam, N. Experimental and theoretical investigation on the effects of lower concentration CeO₂/water nanofluid in flat-plate solar collector. *J. Anal. Calorim.* **2019**, *135*, 29–44. [[CrossRef](#)]
29. Zhao, Y.; Zhang, Z.; Shi, L.; Zhang, F.; Li, S.; Zeng, R. Corrosion resistance of a self-healing multilayer film based on SiO₂ and CeO₂ nanoparticles layer-by-layer assembly on Mg alloys. *Mater. Lett.* **2019**, *237*, 14–18. [[CrossRef](#)]

30. Kumar, P.M.; Mylsamy, K.; Prakash, K.B.; Nithish, M.; Anandkumar, R. Investigating thermal properties of Nanoparticle Dispersed Paraffin (NDP) as phase change material for thermal energy storage. *Mater. Today-Proc.* **2020**. [[CrossRef](#)]
31. Karimzadehkhoei, M.; Shojaeian, M.; Şendur, K.; Mengüç, M.P.; Koşar, A. The effect of nanoparticle type and nanoparticle mass fraction on heat transfer enhancement in pool boiling. *Int. J. Heat Mass Tran.* **2017**, *109*, 157–166. [[CrossRef](#)]
32. Kumar, P.M.; Anandkumar, R.; Sudarvizhi, D.; Mylsamy, K.; Nithish, M. Experimental and Theoretical Investigations on Thermal Conductivity of the Paraffin Wax using CuO Nanoparticles. *Mater. Today-Proc.* **2020**, *22*, 1987–1993. [[CrossRef](#)]
33. Kumar, P.M.; Mylsamy, K. Experimental investigation of solar water heater integrated with a nanocomposite phase change material. *J. Therm. Anal. Calorim.* **2019**, *136*, 121–132. [[CrossRef](#)]
34. George, M.; Pandey, A.K.; Abd Rahim, N.; Tyagi, V.V.; Shahabuddin, S.; Saidur, R. A novel polyaniline (PANI)/paraffin wax nano composite phase change material: Superior transition heat storage capacity, thermal conductivity and thermal reliability. *Sol. Energy* **2020**, *204*, 448–458. [[CrossRef](#)]
35. Amin, M.; Putra, N.; Kosasih, E.A.; Prawiro, E.; Luanto, R.A.; Mahlia, T.M.I. Thermal properties of beeswax/graphene phase change material as energy storage for building applications. *Appl. Eng.* **2017**, *112*, 273–280. [[CrossRef](#)]
36. Battisha, I.K.; El Beyally, A.; El Mongy, S.A.; Nahrawi, A.M. Development of the FTIR properties of nano-structure silica gel doped with different rare earth elements, prepared by sol-gel route. *J. Sol-Gel Sci. Technol.* **2007**, *41*, 129–137. [[CrossRef](#)]
37. Miri, A.; Sarani, M. Biosynthesis, characterization and cytotoxic activity of CeO₂ nanoparticles. *Ceram. Int.* **2018**, *44*, 12642–12647. [[CrossRef](#)]
38. Lin, S.C.; Al-Kayiem, H.H. Evaluation of copper nanoparticles–Paraffin wax compositions for solar thermal energy storage. *Sol. Energy* **2016**, *132*, 267–278. [[CrossRef](#)]
39. Fan, L.W.; Fang, X.; Wang, X.; Zeng, Y.; Xiao, Y.Q.; Yu, Z.T.; Xu, X.; Hu, Y.C.; Cen, K.F. Effects of various carbon nanofillers on the thermal conductivity and energy storage properties of paraffin-based nanocomposite phase change materials. *Appl. Energ.* **2013**, *110*, 163–172. [[CrossRef](#)]
40. Sahan, N.; Paksoy, H. Investigating thermal properties of using nano-tubular ZnO powder in paraffin as phase change material composite for thermal energy storage. *Compos. Part B-Eng.* **2017**, *126*, 88–93. [[CrossRef](#)]
41. Li, Y.; Li, J.; Deng, Y.; Guan, W.; Wang, X.; Qian, T. Preparation of paraffin/porous TiO₂ foams with enhanced thermal conductivity as PCM, by covering the TiO₂ surface with a carbon layer. *Appl. Energ.* **2016**, *171*, 37–45. [[CrossRef](#)]
42. Jiang, X.; Luo, R.; Peng, F.; Fang, Y.; Akiyama, T.; Wang, S. Synthesis, characterization and thermal properties of paraffin microcapsules modified with nano-Al₂O₃. *Appl. Energ.* **2015**, *137*, 731–737. [[CrossRef](#)]
43. Kumar, P.M.; Mylsamy, K. A comprehensive study on thermal storage characteristics of nano-CeO₂ embedded phase change material and its influence on the performance of evacuated tube solar water heater. *Renew. Energ.* **2020**. [[CrossRef](#)]
44. Hamid, K.A.; Azmi, W.H.; Nabil, M.F.; Mamat, R.; Sharma, K.V. Experimental investigation of thermal conductivity and dynamic viscosity on nanoparticle mixture ratios of TiO₂-SiO₂ nanofluids. *Int. J. Heat Mass Tran.* **2018**, *116*, 1143–1152. [[CrossRef](#)]
45. Abdollahzadeh, J.M.; Park, J.H. Effects of brownian motion on freezing of PCM containing nanoparticles. *Therm. Sci.* **2016**, *20*, 1533–1541. [[CrossRef](#)]

